

## PHYSICS INVESTIGATION

# Feasibility of spinal stereotactic body radiotherapy in Elekta Unity<sup>®</sup> MR-Linac

Eun Young Han, PhD<sup>1</sup>, Manik Aima, PhD<sup>1</sup>, Neil Hughes, BSRT<sup>2</sup>, Tina M. Briere, PhD<sup>1</sup>, Debra N. Yeboa, MD<sup>2</sup>, Pam Castillo, BS, CMD<sup>2</sup>, Jihong Wang, PhD<sup>1</sup>, Jinzhong Yang, PhD<sup>1</sup> and Sastry Vedam, PhD<sup>1</sup>

<sup>1</sup>Department of Radiation Physics, University of Texas MD Anderson Cancer Center, Houston, TX, USA

<sup>2</sup>Department of Radiation Oncology, University of Texas MD Anderson Cancer Center, Houston, TX, USA

*Correspondence to: Eun Young Han, Department of Radiation Physics, Unit 94, University of Texas MD Anderson Cancer Center, 1515 Holcomb Blvd, Houston, TX 77030, USA; email: ehan@mdanderson.org; Phone: +1 (713) 563-2555*

*(Received: March 12, 2020; Accepted: June 2, 2020)*

## ABSTRACT

The Elekta Unity MR-Linac (MRL) is expected to benefit spine stereotactic body radiotherapy (SBRT) due to the improved soft tissue contrast available with onboard MR imaging. However, the irradiation geometry and beam configuration of the MRL deviates from the conventional linear accelerator (Linac). The purpose of the study was to investigate the feasibility of spine SBRT on the MRL. Treatment plans were generated for lumbar and thoracic spines. Target and spinal cord doses were measured with two cylindrical ion chambers inserted into an anthropomorphic spine phantom. Our study indicated that the Monaco treatment planning system (TPS) could generate clinical treatment plans for the MRL that were of comparable quality to the RayStation TPS with a conventional Linac. For both Linacs the planned dose within the gross tumor volume agreed with measurements within  $\pm 3\%$ . For the spinal cord, while the measured doses from the TrueBeam were 1.8% higher for the lumbar spine plan and 6.9% higher for thoracic spine plan, the measured doses from MRL were 0.6% lower for the lumbar spine plan and 3.9% higher for the thoracic spine plan. In conclusion, the feasibility of spine SBRT in Elekta Unity MRL has been demonstrated, however, more effort is needed for such as optimizing the online plan adaptation method.

**Keywords:** Spine SBRT, Unity MR-Linac, TrueBeam

## INTRODUCTION

Hypo-fractionated spine stereotactic body radiotherapy (SBRT) has been demonstrated to be an important radiotherapy treatment option for spinal metastases. [1, 2] An inherent challenge in treatment planning and delivery of spine SBRT is protection of a spinal cord, which is one of serial organs.[1] This requires a highly conformal dose distribution in the target volume and a

steep dose fall-off in the spinal cord to achieve the spinal cord dose constraints. Target dose coverage is often compromised in order to meet the spinal cord dose constraints during radiotherapy treatment planning, especially when the target volume abuts the spinal cord. At our institution, spine SBRT treatments have been delivered by a conventional linear accelerator (Linac), together with the ExacTrac x-ray localization system (v6.2.1; BrainLab, Munich, Germany). ExacTrac uses a

high-resolution stereoscopic x-ray imaging system and an infrared optical system to detect and align the patient position.

Recently, the Elekta Unity MR-Linac (MRL; Stockholm, Sweden), integrating a 1.5 Tesla (T) Philips magnetic resonance imaging system (MRI; Amsterdam, Netherlands) and an Elekta 7-MV Linac, was commissioned at our institution.[3-8] The feasibility of SBRT delivery using the MRL system has been evaluated for various treatment sites, including pelvic node oligometastases[9], brain metastases[10], retroperitoneal metastases[11], and lung cancer[12]. The MRL is expected to enhance spine SBRT because improved soft tissue contrast with the onboard MRI, online daily target and spinal cord delineation, and real-time spinal cord visibility help reduce setup and intra-fractional motion uncertainties. However, the irradiation geometry and beam configuration of the MRL deviate from those clinically implemented with a conventional Linac.

Besides, the Electron Return Effect (ERE) is a physical phenomenon unique to the MRL. Under the influence of the 1.5 T magnetic field, secondary electrons in air or a low density medium can be deflected by the Lorentz force and cause increased dose to neighboring tissue.[5, 13] For thoracic spine SBRT, the ERE might occur between the lungs and spine vertebra. Therefore, before spine SBRT with the MRL can be clinically implemented, it is important to validate the feasibility of the treatment planning and delivery, especially, given the cord dose constraints [14] and target dose coverage compared to the conventional Linac-based treatments.[15, 16]

The purpose of the study was to investigate the feasibility of spine SBRT with the MRL. Treatment plans were generated for lumbar and thoracic spines. Target and spinal cord doses were measured with two cylindrical ion chambers delivered with a TrueBeam STx (v2.0, Varian Medical Systems, Palo Alto, CA) and Elekta Unity MRL. An MR-compatible anthropomorphic spine phantom was used for the entire treatment chain including planning CT imaging, pre-treatment set-up, MR-based image guidance and treatment delivery. To the best of our knowledge, this is the first study comparing the treatment delivery of spine SBRT with the 1.5 T MRL to the conventional Linac.

**METHODS**

*RTsafe Spine phantom*

We used an anthropomorphic pediatric spine phantom (10-year-old female, RTsafe, Artotinis, Greece) that contains three consecutive spine vertebral bodies (lumbar spine 3-5) with bone-equivalent density. The size of the

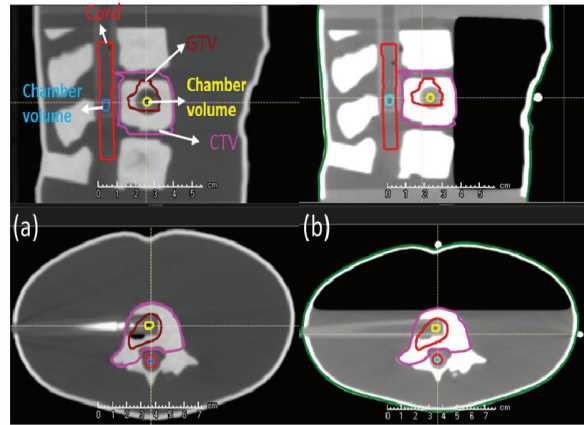


**Figure 1.** Sagittal (top) and axial (bottom) views of CT images and contoured structures in the Spine phantom (a) Completely water-filled phantom to simulate a lumbar spine setup. (b) Partially filled phantom to simulate a thoracic spine setup. GTV, gross tumor volume; CTV, clinical target volume.

phantom is 21 cm wide, 11.5 cm tall, and 11.1 cm long. It accommodates two ionization chambers into the spinal canal and central spine vertebra. The cylindrical ionization chamber inserts were made of 2 mm thick polymethyl methacrylate (PMMA). The phantom was filled either partially or completely with water prior to imaging or treatment delivery (Figures 1-2).

*Plan generation*

Two consecutive computed tomography (CT) scans (1-mm slice thickness) were acquired: one with the completely water-filled phantom mimicking the lumbar spine and the other with the phantom partially filled up to the anterior border of the vertebral bodies to mimic the thoracic spine. The water levels were selected so that the chamber in the gross tumor vol-

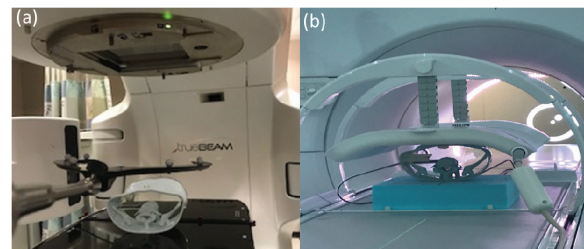


**Figure 2.** Phantom placement during irradiation. (a) Phantom placement in the Varian TrueBeam with ExacTrac reference array. (b) Elekta Unity MR-Linac with body coil placed above the phantom sitting on top of 7.5cm thick polystyrene foam.

ume (GTV) was completely submerged in water as shown in Figure 1(b).

The contours were drawn by an ABR-certified radiation oncologist in RayStation (v8, RaySearch, Stockholm, Sweden). The GTV was drawn in the central vertebra in which the chamber was located. The body of the central vertebra, right pedicle and right transverse process were included in the clinical target volume (CTV) following Spine Radiosurgery Consortium Guidelines.[17] The inner wall of the chamber insert in the spinal canal was considered to be a spinal cord. The two sensitive volumes of chambers were outlined on the CT image. The CT images and structure set were exported from the RayStation treatment planning system (TPS) to the Monaco TPS (v 5.4, Elekta AB, Stockholm, Sweden).

The prescription dose of the GTV was 24 Gy (single fraction) with the optimization goals of V100%  $\geq$  95% (at least 95% of the GTV to be covered by the prescription dose), maximum dose (Dmax)  $\leq$  120% of the prescription dose and minimum dose (Dmin)  $\geq$  15 Gy.[18] The prescription dose of the CTV was 16 Gy with the goal of V100%  $\geq$  95%. Dose constraints for the spinal cord were V10Gy  $\leq$  1cm<sup>3</sup> (volume of the spinal cord receiving 10 Gy should be less than 1cm<sup>3</sup>) and Dmax  $\leq$  12 Gy. All plans were normalized so that at least 95% of the CTV were covered by the prescribed dose (16 Gy).

The calculation dose grid size was set to 2 mm for both planning systems. The lumbar spine and thoracic spine plans were generated by two experienced dosimetrists. One dosimetrist with more than 10 years' experiences planned on RayStation TPS and the other dosimetrist with more than 3 years' experiences planned on Monaco TPS since our Unity was commissioned in 2018. The plans were optimized to yield the best possible plans, which were then reviewed by the radiation oncologist. The RayStation plans were compared with the Monaco plans using the plan quality index, which included target coverage, Paddick conformity index, gradient index, homogeneity index, R50 (to evaluate the impact of intermediate dose on normal tissues), V10Gy and Dmax to the spinal cord, beam-on-time and total monitor units (MU). The Paddick conformity index was calculated as

$$\frac{TV_{PIV^2}}{TV \times PV_{100\%}}$$

where TV<sub>PIV</sub> represents the target volume covered by the prescription isodose volume, PV<sub>100%</sub> represents the patient volume covered by the prescribed dose, and TV is the target volume. The gradient index was calculated as

$$\frac{PV_{50\%}}{PV_{100\%}}$$

where PV<sub>50%</sub> represents the patient volume covered by 50% of the prescribed dose. The homogeneity index was calculated as the maximum target dose divided by the prescription dose. Finally, R50 is a ratio of PV<sub>50%</sub> to the target volume.

The RayStation plans were created for the TrueBeam with 6 MV flattening-filtered photon beams and 120 high definition MLC leaf pairs with a 2.5-mm leaf width at isocenter (100.0 cm SSD) within the central 8-cm field and 5.0 mm beyond. The step-and-shoot IMRT treatment technique was employed with coplanar gantry angles - 200, 220, 240, 260, 100, 120, 140, 160, and 180. The collapsed cone convolution (CCC) dose calculation method was used. A maximum of 50 segments per plan, a minimum of 2.0 MU per segment and a minimum segment width of 4.0 cm<sup>2</sup> were allowed during the plan optimization.

The Monaco plans were created for the MRL with 7 MV flattening-filter free photon beams and 80 MLC leaf pairs with a leaf width of 7.2 mm at isocenter (143.5 cm SSD).[4] The MRL isocenter is fixed at the center of the bore, which is 14 cm above the couch top. A 7.5-cm polystyrene foam block was placed under the phantom in order to raise the phantom to isocenter-level. The same numbers of beams were employed as the RayStation plans but angles (200, 225, 260, 280, 85, 105, 140, 160, and 180) were modified to avoid the high-density materials at the edge of the MRL couch. Monte Carlo dose calculations were performed at < 1% per calculation statistical uncertainty. A fast graphic processing unit based Monte Carlo dose (GPUMCD) calculation method was used [19]. A maximum of 100 segments per plan, a minimum of 2.0 MU per segment and a minimum segment area of 2.0 cm<sup>2</sup> were allowed during the plan optimization.

### Measurement comparison

The pretreatment setup in the TrueBeam was performed as follows: the phantom's initial position was corrected within the tolerance of 0.7 mm and 0.8 degrees by the 6 degree-of-freedom (DOF) Varian image-guided radiation therapy (IGRT) couch controlled by the Exactrac. The set up was verified by on-board Varian cone-beam CT (CBCT), as is used to treat the actual spine SBRT patients (Figure 2a).

Dose measurements were performed with two Exradin A1SLMR chambers (Standard imaging, Middleton, WI) inserted into the GTV and the spinal cord chamber inserts at the same time. Both ADCL-calibrated cham-

bers were connected to a two-channel electrometer (PE electrometer, Sun Nuclear, Orlando, FL). Each plan was measured three times on different dates to verify the measurement reproducibility. Absolute dose calculations were performed based on AAPM Task Group 51 and its addendum. The energy-dependent correction factor ( $k_q$ ) was estimated as 0.992, assuming water-equivalent homogeneity inside the phantom.[20, 21] The TrueBeam machine output was also measured using a 1D water tank (Sun Nuclear, Melbourne, FL) and Farmer type chamber (PTW-Freiburg GmbH, Freiburg, Germany; sensitive volume: 0.6 cm<sup>3</sup>) following TG-51 for comparison. The absolute doses from both Exradin chambers were within 1.2% of the dose from the PTW Farmer chamber. This indicated the measurement uncertainty of the two Exradin chambers for absolute dosimetry in a zero magnetic field environment.

The pretreatment setup for the MRL was as follows: first, the T2-weighted images of the anthropomorphic phantom were obtained using the following parameters: 300 slices with a field of view of 400 x 400 x 300 mm<sup>3</sup>, reconstructed voxel size of 0.83 x 0.83 x 1.0 mm<sup>3</sup>, and T2-weighted repetition time/echo time of 1535 ms / 278 ms. The scan duration was 2 minutes. The T2-weighted MR image was then automatically imported into online Monaco TPS (Figure 2b).

Once the T2 image was registered with the planning CT image, the isocenter shift was determined and the adapted plan was generated. Instead of adjusting the treatment couch, a virtual isocenter shift was performed by creating the adapted plan using the “adapt-to-position” workflow available with the Elekta Unity. In this workflow, the re-delineation of the target is not required and the dose of the original plan is considered as the target dose in the objective function.[22]

Two chambers could not be used at the same time in the MRL due to technical difficulties, and therefore the GTV and cord doses were measured separately with two different adapted plans. Absolute dose calculations were based on AAPM Task Group 51 and other references and a  $k_q$  factor of 0.986 was used assuming water-equivalent homogeneity within the phantom.[21, 23]

## RESULTS

### Plan comparison

Table 1 shows the results for the 4 plans: Monaco generated lumbar spine plan (MRL\_LS), Monaco generated thoracic spine plan (MRL\_TS), RayStation generated lumbar spine plan (RS\_LS) and RayStation generated thoracic spine plan (RS\_TS). All 4 plans met the planning goals. Target coverage and spinal cord

**Table 1. Comparison of Monaco-generated and RayStation-generated plans**

Variable	MRL_LS	RS_LS	MRL_TS	RS_TS
GTV				
D95%, cGy	2402.1	2485.0	2348.8	2437.0
Minimum dose, cGy	2277.5	2321.0	2186.5	2175.0
Maximum dose, cGy	2729.3	2759.0	2651.8	2737.0
Conformity index	0.6	0.4	0.7	0.4
Homogeneity index	1.1	1.1	1.1	1.1
R50	25.9	27.9	28.1	24.9
CTV				
D95%, cGy	1600.3	1601.0	1602.8	1600.0
Conformity index	0.8	0.8	0.9	0.8
Homogeneity index	1.7	1.7	1.7	1.7
Gradient index	3.7	3.8	3.4	3.4
R50	4.09	4.28	4.09	3.78
Spinal cord				
Maximum dose, cGy	1042.4	1065.0	1109.3	1032.0
V10Gy, cm <sup>3</sup>	0.01	0.01	0.059	0.0
Beam-on time, minutes	13.0	8.1	12.7	7.5
Monitor units	5517.4	4869.3	5390.3	4522.6

MRL\_LS, Monaco-generated lumbar spine plan; RS\_LS, RayStation-generated lumbar spine plan; MRL\_TS, Monaco-generated thoracic spine plan; RS\_TS, RayStation-generated thoracic spine plan; GTV, gross tumor volume; CTV, clinical target volume

dose were similar and other plan quality indicators including Paddick conformity index, gradient index, and homogeneity index were also comparable. The beam on times for TrueBeam plans were 7.5-8.1 min compared to 12.7-13.0 min for the MRL. This is due to the increased number of MUs with the MRL plans as well as the lower dose rate (425 MU/min for the MRL compared to 600 MU/min for the TrueBeam). The MRI scan time for pretreatment setup was 2 min compared to 1.5 min for Exactrac X-ray and CBCT.

### Pretreatment setup

Figure 3 displays the pretreatment setup for TrueBeam delivery. The initial position was corrected by Exactrac



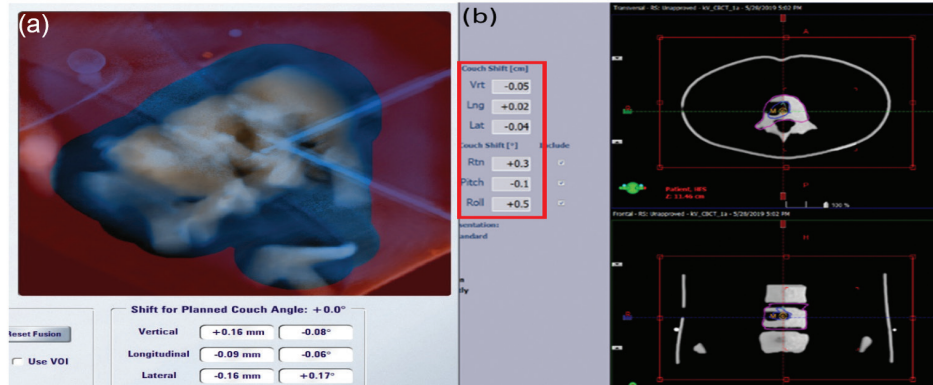


**Figure 3.** Pretreatment setup displays for Varian TrueBeam delivery. (a) BrainLab ExacTrac. (b) Verification by cone beam computed tomography.

followed by CBCT verification, which reflects the typical clinical workflow at our institution. Residual shifts following the image registration were  $\leq 0.5$  mm and  $\leq 0.5^\circ$ .

Figure 4 shows the image registration of the daily T2 image and planning CT images. After the T2 image was manually or automatically registered to the planning CT, an adapted plan was generated and compared with the original plan. The adapted plan was then exported to the MRL treatment console for delivery after plan review. If the dose constraints of the spinal cord was not met, the adapted plan was re-normalized. Figure 5 shows an example of the cumulative DVH for the plan comparison between the original plan and the daily adapted plan.

### Measurement comparison

Ionization chamber measurements within the GTV for the RS\_LS plan agreed with the original plan within -1.4% and cord chamber measurements were within 1.8%. For the RS\_TS plan, measurements in the GTV were within -2.6% and the cord agreed within 6.9% with the original plan.

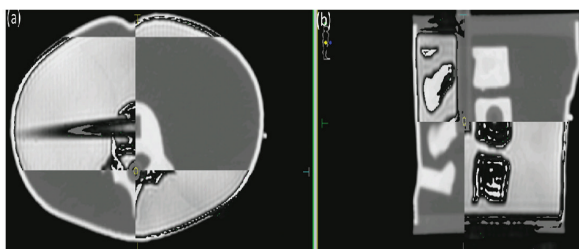


**Figure 4.** Planning computed tomography image and daily magnetic resonance (T2) image registration for pretreatment setup in the Elekta Unity MR-Linac. (a) Axial plane. (b) Sagittal plane.

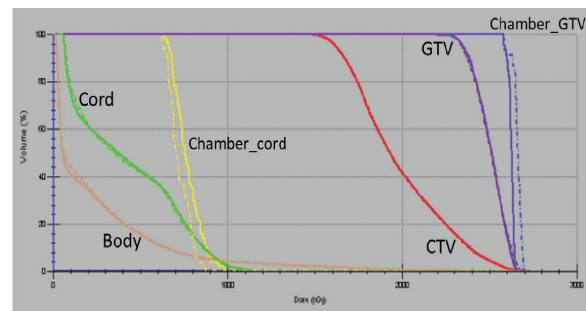


**Figure 5.** Cumulative dose volume histogram for a sample plan. A comparison is shown between the original plan (dotted line) and the adapted plan (solid line). GTV, gross tumor volume; CTV, clinical target volume.

Ionization chamber measurements within the GTV for the MRL\_LS plan agreed with the original plan within 1.2% and cord chamber measurements were within -0.6%. For the MRL\_TS plan, measurements in the GTV were within 3.1% and measurements in the cord agreed within 3.9% comparing to the original plan. Table 2 shows the detailed measurement comparison between the RayStation and Monaco lumbar and thoracic spine plans.

The mean doses of the chamber volume in the spinal cord were higher in Monaco plans than those of RayStation plans because the dose constraints of the spinal cord ( $D_{max}$  and  $V_{10Gy}$ ) were already met and the chamber volume was not specifically included in the optimization parameters.

### Discussion

In this study four treatment plans for spine SBRT were generated - lumbar and thoracic spine plans using

**Table 2. Comparison of measurements obtained by TrueBeam and MRL plans**

Variable	Dmean, cGy			
	Lumbar spine		Thoracic spine	
	GTV	Spinal cord	GTV	Spinal cord
RayStation				
Measurement	2605.2 ± 17.4	514.3 ± 2.7	2595.5 ± 9.6	470.4 ± 3.4
Original plan	2641.0	505.0	2664.0	440.0
% difference	-1.4	1.8	-2.6	6.9
Monaco				
Measurement	2702.9 ± 113.9	601.8 ± 22.9	2684 ± 14.4	884.6 ± 37.4
Adapted plan	2671.3 ± 19.6	605.6 ± 15.6	2602.3 ± 5.8	851.3 ± 39.6
Original plan	2644.5	562.8	2595.5	788.5
% difference <sup>†</sup>	1.2	-0.6	3.1	3.9

<sup>†</sup>% difference = (Measurement – (Adapted plan)) × 100 / Adapted plan

the RayStation and Monaco TPSs and delivered with a Varian TrueBeam and Elekta Unity MRL, respectively. The spinal cord and target doses were measured by two cylindrical ion chambers and compared with the respective plans. The current study was the first feasibility study in which doses to the target and the spinal cord were actually measured by two ion chambers with a MR-compatible anthropomorphic phantom.

Our study showed that the Monaco TPS could generate clinical treatment plans comparable to the RayStation TPS for spine SBRT. Elsewhere in the literature, Yadav et al reported that ViewRay MRIdian Linac plans (Oakwood Village, Ohio) achieved equivalent target coverage and spinal cord dose compared to Pinnacle generated plans for a Varian TrueBeam.[16] Choi et al have shown that dose to the spinal cord for IMRT plans using the ViewRay MRL was the lowest among other types of plans including the ViewRay MR Co<sub>60</sub> and VMAT with a TrueBeam.[15]

In our study, regardless of machines, the planned dose for the chamber in the GTV was measured within ±3%. For the spinal cord, the measured doses with the MRL plans agreed better than the RayStation plans and the measurements in the lumbar spine agreed better with plans than those in the thoracic spine. The TG-51 is meant for use in a homogeneous water phantom under conditions of electronic equilibrium, therefore, applying it to a measurement in the inhomogeneous thoracic spine phantom might probably have contributed some uncertainties.

There are a few uncertainties involved in the MRL treatment work flow compared with those of the TrueBeam, as detailed below.

First, in the MRL plan, the mean dose of the cord chamber volume in the adapted plans increased by

up to 8.0 % compared to the original plans. For both lumbar and thoracic spine plans, we later attempted to include the cord chamber volume plus a 2 mm margin in the Monaco optimization process to reduce the dose gradient near the cord chamber volume but this did not impact the mean dose increase after the plan adaptation. This could be a limiting factor of the plan adaptation workflow for the plan with the highly steep dose fall-off near the spinal cord. Winkle et al reported that the full online re-planned treatment plan showed the most favorable DVH comparison with the original plan; therefore, it could be beneficial to optimize the most appropriate plan adaptation workflow for spine SBRT planning.[24]

Secondly, our results may be limited to the specific plans used in this study and could be changed by different configurations of a GTV/CTV and a spinal cord of real patients. Lastly, according to O'Brien et al, the magnetic field correction factor varies in magnitude by the Farmer type chamber orientation, with the smallest corrections (< 0.5%) found when the chamber was parallel to the magnetic field (in our case, for the chamber in the cord). The perpendicular orientation to the magnetic field (in our case for the chamber in the GTV) required a correction of ~4%.[25] However, we did not apply those factors because they included the Farmer type chambers only with a sensitive volume of 0.6 cm<sup>3</sup> and their beam (Gantry 0) was perpendicular to both the chamber and the magnetic field lines. In another study, O'Brien and Sawakuchi studied the chamber-phantom air gap effect in a 1.5 T magnetic field using Monte Carlo calculations and concluded that there was 1.6% dose difference caused by the presence of a 0.2 mm thick asymmetric air gap between the chamber and phantom.[26] However, our chamber inserts were spe-

cifically made to conform to the shape of our ionization chamber therefore it was not necessary to apply their correction factor.

## CONCLUSION

We found that the Monaco TPS for the Elekta Unity MRL can generate the plans comparable to the RayStation TPS and the Monaco-planned doses for the chamber in the GTV were measured within  $\pm 3\%$  accuracy and those for the chamber in the spinal cord were measured within  $\pm 4\%$  accuracy. In conclusion, the feasibility of spine SBRT in Elekta Unity MRL has been demonstrated, however, more effort is needed for such as optimizing the online plan adaptation method.

## ACKNOWLEDGEMENTS

The authors thank Erica Goodoff in Scientific Publications, Research Medical Library at the University of Texas MD Anderson Cancer Center for editing this manuscript. The authors wish to thank RTsafe for lending us the Spine phantom, as well as Standard Imaging for lending us an Exradin A1SLMR chamber. Authors thank Dr. Daniel O'Brien in Elekta for his helpful comments.

### *Authors' disclosure of potential conflicts of interest*

The authors have nothing to disclose

### *Author contributions*

Conception and design: Eun Young Han  
 Data collection: Eun Young Han, Manik Aima, Neil Hughes, and Pam Castillo  
 Data analysis and interpretation: Eun Young Han, Manik Aima, and Jinzhong Yang  
 Manuscript writing: Eun Young Han  
 Manuscript review: Tina M. Briere, Debra N. Yeboa, Jihong Wang, Jinzhong Yang, and Sastry Vedam  
 Final approval of manuscript: Sastry Vedam

## REFERENCES

- Ryu S, Pugh SL, Gerszten PC, Yin F-F, Timmerman RD, Hitchcock YJ, Movsas B, Kanner AA, Berk LB, Followill DS, Kachnic LA. RTOG 0631 phase 2/3 study of image guided stereotactic radiosurgery for localized (1-3) spine metastases: phase 2 results. *Practical Radiation Oncology*. 2014;4(2):76-81. Epub 06/04. doi: 10.1016/j.prro.2013.05.001. PubMed PMID: 24890347.
- Chang EL, Shiu AS, Mendel E, Mathews LA, Mahajan A, Allen PK, Weinberg JS, Brown BW, Wang XS, Woo SY, Cleeland C, Maor MH, Rhines LD. Phase I/II study of stereotactic body radiotherapy for spinal metastasis and its pattern of failure. *Journal of neurosurgery Spine*. 2007;7(2):151-60. Epub 2007/08/11. doi: 10.3171/spi-07/08/151. PubMed PMID: 17688054.
- Raaijmakers BW, Lagendijk JJ, Overweg J, Kok JG, Raaijmakers AJ, Kerkhof EM, van der Put RW, Meijnsing I, Crijns SP, Benedosso F, van Vulpen M, de Graaff CH, Allen J, Brown KJ. Integrating a 1.5 T MRI scanner with a 6 MV accelerator: proof of concept. *Physics in Medicine and Biology*. 2009;54(12):N229-37. Epub 2009/05/20. doi: 10.1088/0031-9155/54/12/n01. PubMed PMID: 19451689.
- Raaijmakers AJ, Hardemark B, Raaijmakers BW, Raaijmakers CP, Lagendijk JJ. Dose optimization for the MRI-accelerator: IMRT in the presence of a magnetic field. *Physics in Medicine and Biology*. 2007;52(23):7045-54. Epub 2007/11/22. doi: 10.1088/0031-9155/52/23/018. PubMed PMID: 18029992.
- Raaijmakers AJ, Raaijmakers BW, Lagendijk JJ. Integrating a MRI scanner with a 6 MV radiotherapy accelerator: dose increase at tissue-air interfaces in a lateral magnetic field due to returning electrons. *Physics in Medicine and Biology*. 2005;50(7):1363-76. Epub 2005/03/31. doi: 10.1088/0031-9155/50/7/002. PubMed PMID: 15798329.
- Raaijmakers AJ, Raaijmakers BW, Lagendijk JJ. Experimental verification of magnetic field dose effects for the MRI-accelerator. *Physics in Medicine and Biology*. 2007;52(14):4283-91. Epub 2007/08/01. doi: 10.1088/0031-9155/52/14/017. PubMed PMID: 17664608.
- Raaijmakers AJ, Raaijmakers BW, Lagendijk JJ. Magnetic-field-induced dose effects in MR-guided radiotherapy systems: dependence on the magnetic field strength. *Physics in Medicine and Biology*. 2008;53(4):909-23. Epub 2008/02/12. doi: 10.1088/0031-9155/53/4/006. PubMed PMID: 18263948.
- Raaijmakers AJ, Raaijmakers BW, van der Meer S, Lagendijk JJ. Integrating a MRI scanner with a 6 MV radiotherapy accelerator: impact of the surface orientation on the entrance and exit dose due to the transverse magnetic field. *Physics in Medicine and Biology*. 2007;52(4):929-39. Epub 2007/02/01. doi: 10.1088/0031-9155/52/4/005. PubMed PMID: 17264362.
- Werensteijn-Honingh AM, Kroon PS, Winkel D, Aalbers EM, van Asselen B, Bol GH, Brown KJ, Eppinga WSC, van Es CA, Glitzner M, de Groot-van Breugel EN, Hackett SL, Intven M, Kok JGM, Kontaxis C, Kotte AN, Lagendijk JJW, Philippens MEP, Tijssen RHN, Wolthaus JWH, Woodings SJ, Raaijmakers BW, Jurgenliemk-Schulz IM. Feasibility of stereotactic radiotherapy using a 1.5T MR-linac: Multifraction treatment of pelvic lymph node oligometastases. *Radiotherapy and oncology : journal of the European Society for Therapeutic Radiology and Oncology*. 2019;134:50-4. Epub 2019/04/22. doi: 10.1016/j.radonc.2019.01.024. PubMed PMID: 31005224.
- Tseng CL, Eppinga W, Seravalli E, Hackett S, Brand E, Ruschin M, Lee YK, Atenafu EG, Sahgal A. Dosimetric

- feasibility of the hybrid Magnetic Resonance Imaging (MRI)-linac System (MRL) for brain metastases: The impact of the magnetic field. *Radiotherapy and oncology : journal of the European Society for Therapeutic Radiology and Oncology*. 2017;125(2):273-9. Epub 2017/10/29. doi: 10.1016/j.radonc.2017.09.036. PubMed PMID: 29079310.
11. Ghanem AI, Glide-Hurst C, Siddiqui MS, Chetty IJ, Movsas B. Retroperitoneal Metastasis Abutting Small Bowel: A Novel Magnetic Resonance-Guided Radiation Approach. *Cureus*. 2018;10(4):e2412. Epub 2018/06/07. doi: 10.7759/cureus.2412. PubMed PMID: 29872593; PubMed Central PMCID: PMC5984256.
  12. Bainbridge HE, Menten MJ, Fast MF, Nill S, Oelfke U, McDonald F. Treating locally advanced lung cancer with a 1.5T MR-Linac - Effects of the magnetic field and irradiation geometry on conventionally fractionated and isotoxic dose-escalated radiotherapy. *Radiotherapy and Oncology: Journal of the European Society for Therapeutic Radiology and Oncology*. 2017;125(2):280-5. Epub 2017/10/11. doi: 10.1016/j.radonc.2017.09.009. PubMed PMID: 28987747; PubMed Central PMCID: PMC5710994.
  13. Chen X, Prior P, Chen GP, Schultz CJ, Li XA. Technical Note: Dose effects of 1.5 T transverse magnetic field on tissue interfaces in MRI-guided radiotherapy. *Med Phys*. 2016;43(8):4797. Epub 2016/08/05. doi: 10.1118/1.4959534. PubMed PMID: 27487897.
  14. Ryu S, Jin JY, Jin R, Rock J, Ajlouni M, Movsas B, Rosenblum M, Kim JH. Partial volume tolerance of the spinal cord and complications of single-dose radiosurgery. *Cancer*. 2007;109(3):628-36. Epub 2006/12/15. doi: 10.1002/cncr.22442. PubMed PMID: 17167762.
  15. Choi CH, Kim JH, Kim J-I, Park JM. Comparison of treatment plan quality among MRI-based IMRT with a linac, MRI-based IMRT with tri-Co-60 sources, and VMAT for spine SABR. *PLoS One*. 2019;14(7):e0220039. doi: 10.1371/journal.pone.0220039. PubMed PMID: 31329641.
  16. Yadav P, Musunuru HB, Witt JS, Bassetti M, Bayouth J, Baschnagel AM. Dosimetric study for spine stereotactic body radiation therapy: magnetic resonance guided linear accelerator versus volumetric modulated arc therapy. *Radiology and Oncology*. 2019;53(3):362-8. Epub 2019/09/26. doi: 10.2478/raon-2019-0042. PubMed PMID: 31553704; PubMed Central PMCID: PMC6765155.
  17. Cox BW, Spratt DE, Lovelock M, Bilsky MH, Lis E, Ryu S, Sheehan J, Gerszten PC, Chang E, Gibbs I, Soltys S, Sahgal A, Deasy J, Flickinger J, Quader M, Minda S, Yamada Y. International Spine Radiosurgery Consortium consensus guidelines for target volume definition in spinal stereotactic radiosurgery. *Int J Radiat Oncol Biol Phys*. 2012;83(5):e597-605. Epub 2012/05/23. doi: 10.1016/j.ijrobp.2012.03.009. PubMed PMID: 22608954.
  18. Bishop AJ, Tao R, Rebuena NC, Christensen EN, Allen PK, Wang XA, Amini B, Tannir NM, Tatsui CE, Rhines LD, Li J, Chang EL, Brown PD, Ghia AJ. Outcomes for Spine Stereotactic Body Radiation Therapy and an Analysis of Predictors of Local Recurrence. *International Journal of Radiation Oncology • Biology • Physics*. 2015;92(5):1016-26. doi: 10.1016/j.ijrobp.2015.03.037.
  19. Hissoiny S, Ozell B, Bouchard H, Despres P. GPUMCD: A new GPU-oriented Monte Carlo dose calculation platform. *Med Phys*. 2011;38(2):754-64. Epub 2011/04/02. doi: 10.1118/1.3539725. PubMed PMID: 21452713.
  20. McEwen M, DeWerd L, Ibbott G, Followill D, Rogers DWO, Seltzer S, Seuntjens J, Kawachi T, Katayose T, Kodama T, Miyasaka R. Addendum to the AAPM's TG-51 Protocol for Clinical Reference Dosimetry of High-Energy Photon Beams. *Igaku butsuri : Nihon Igaku Butsuri Gakkai kikanishi = Japanese journal of Medical Physics : An Official Journal of Japan Society of Medical Physics*. 2017;37(1):2-24. Epub 2017/09/20. doi: 10.1132/jjimp.37.1\_2. PubMed PMID: 28924094.
  21. Almond PR, Biggs PJ, Coursey BM, Hanson WF, Huq MS, Nath R, Rogers DW. AAPM's TG-51 protocol for clinical reference dosimetry of high-energy photon and electron beams. *Med Phys*. 1999;26(9):1847-70. Epub 1999/10/03. doi: 10.1118/1.598691. PubMed PMID: 10505874.
  22. Ahunbay EE, Ates O, Li XA. An online replanning method using warm start optimization and aperture morphing for flattening-filter-free beams. *Med Phys*. 2016;43(8):4575. Epub 2016/08/05. doi: 10.1118/1.4955439. PubMed PMID: 27487874.
  23. Malkov VN, Rogers DWO. Monte Carlo study of ionization chamber magnetic field correction factors as a function of angle and beam quality. *Med Phys*. 2018;45(2):908-25. Epub 2017/12/09. doi: 10.1002/mp.12716. PubMed PMID: 29218730.
  24. Winkel D, Bol GH, Kiekebosch IH, Van Asselen B, Kroon PS, Jurgenliemk-Schulz IM, Raaymakers BW. Evaluation of online plan adaptation strategies for the 1.5T MR-linac based on "first-in-man" treatments. *Cureus*. 2018;10(4):e2431. Epub 2018/06/08. doi: 10.7759/cureus.2431. PubMed PMID: 29876153; PubMed Central PMCID: PMC5988167.
  25. O'Brien DJ, Roberts DA, Ibbott GS, Sawakuchi GO. Reference dosimetry in magnetic fields: Formalism and ionization chamber correction factors. *Med Phys*. 2016;43(8):4915. Epub 2016/08/05. doi: 10.1118/1.4959785. PubMed PMID: 27487908.
  26. O'Brien DJ, Sawakuchi GO. Monte Carlo study of the chamber-phantom air gap effect in a magnetic field. *Med Phys*. 2017;44(7):3830-8. Epub 2017/04/23. doi: 10.1002/mp.12290. PubMed PMID: 28432792; PubMed Central PMCID: PMC5503156.